Supplementary Information

Mo modulation effect on the hydrogen binding energy of hcp Ru for hydrogen evolution

Zhen Zhang [a, b], Ping Li [d], Qi Wang [b], Qi Feng [a, b], Youkun Tao [c], Jiaoyan Xu [b], Cheng Jiang [b], Xiner Lu [b], Jiantao Fan [b], Meng Gu [b], Hui Li [b *], Haijiang Wang [c *]

a *School of Materials Science and Engineering, Harbin Institute of Technology, Harbin, 150001, China*

b *Department of Materials Science and Engineering, Southern University of Science and Technology, Shenzhen, 518055, China*

c *Department of Mechanical and Energy Engineering, Southern University of Science and Technology, Shenzhen, 518055, China*

d *Department of Physics, Soochow University, Suzhou 215006, China*

* Corresponding author: Department of Materials Science and Engineering, Southern University of Science and Technology, Shenzhen, 518055, China

E-mail address: hui.li@sustc.edu.cn

Table S1. The adsorption energy of H species (ΔE_{H*}), the relevant contributions to the free-energy (ΔZPE and $T\Delta S$), and the final calculated Gibbs free-energy of adsorbed H* (ΔG_{H*}) for different models.

Species	**ΔE_{H*}(eV)**	**ΔZPE(eV)**	**-TΔS (eV)**	**ΔG_{H*} (eV)**
H_2	/	0.289	-0.410	/
H* on pristine Ru	-0.619	0.975	0.205	0.56
H* on Ru site [Mo-Ru]	-1.249	0.686	0.205	-0.36
H* on Mo site [Mo-Ru]	-1.203	0.686	0.205	-0.31
H* on Ru site [$MoRu_3$]	-1.186	0.774	0.205	-0.21
H* on Mo site [$MoRu_3$]	-1.078	0.774	0.205	-0.10

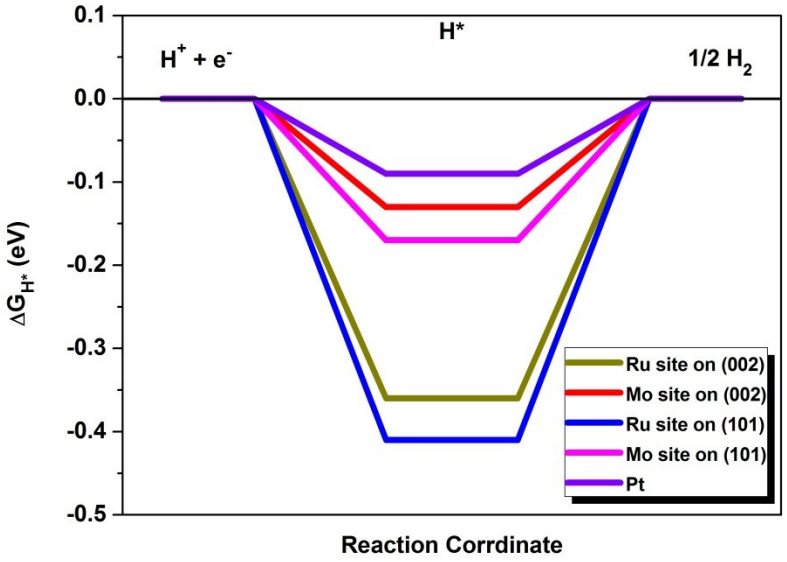

Figure S1. The corresponding values of ΔG_{H*} on the (002) and (101) planes of hcp $MoRu_3$ for Ru and Mo sites. The (002) plane shows Gibbs free energy of adsorption of -0.36 and -0.13 eV for Ru and Mo site, respectively. The (101) plane represents ΔG_{H*} of -0.41 and -0.17 eV for Ru and Mo atom, respectively.

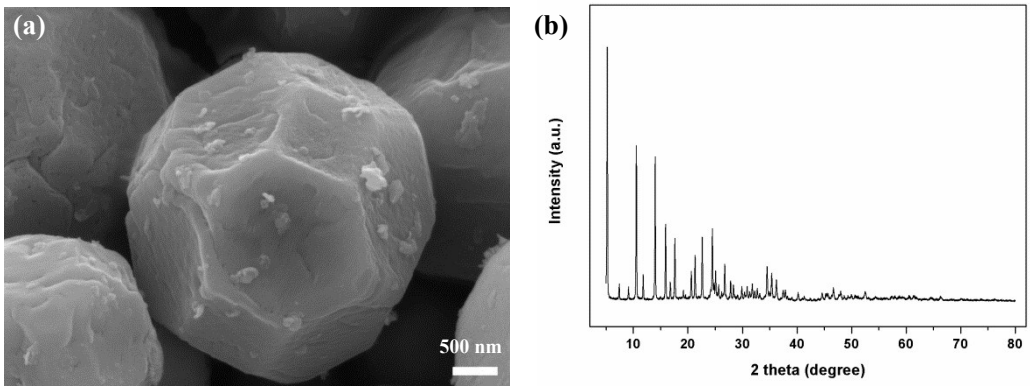

Figure S2. (a) SEM image and (b) XRD pattern of Zn-MOF precursor.

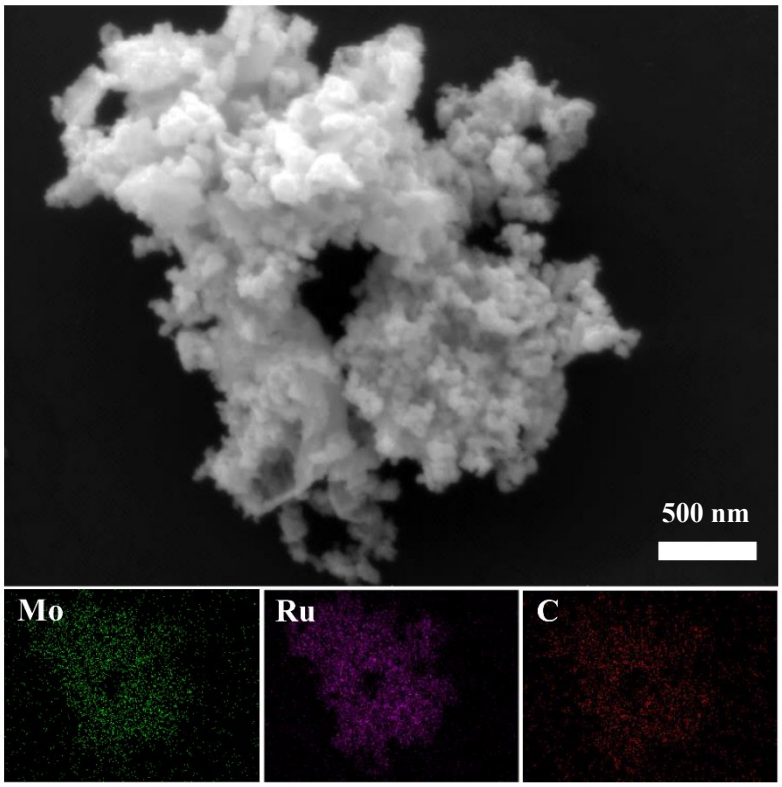

Figure S3. SEM and EDS mapping for Mo@Ru-5.

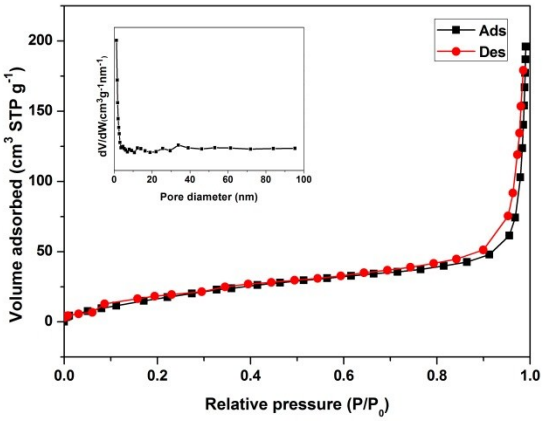

Figure S4. The N_2 adsorption-desorption isotherm and pore size information for Mo@Ru-3. A type- II isotherm with a H3-type hysteresis loop is obtained, which is characteristic of mesoporous non-rigid aggregates. The Mo@Ru-3 sample shows a specific surface area of 71.13 m^2 g^{-1}.

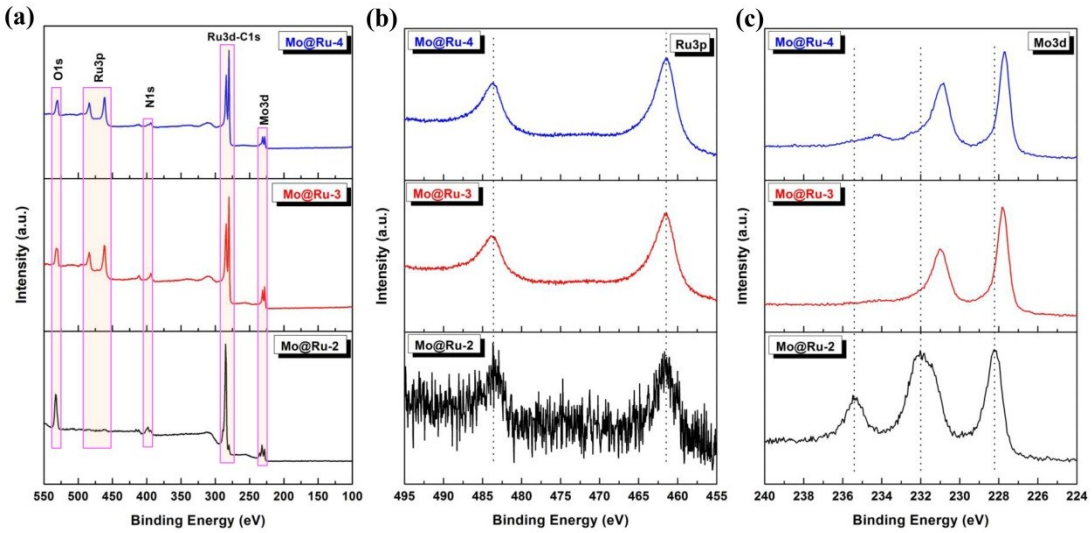

Figure S5. (a) Summarized XPS spectra and (b) Ru3p, (c) Mo3d analysis.

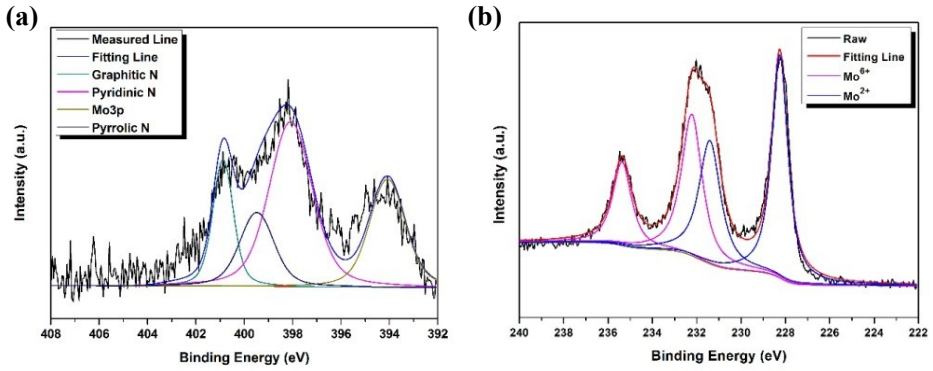

Figure S6. (a) N1s XPS spectrum and (b) Mo3d XPS spectrum of Mo@Ru-2.

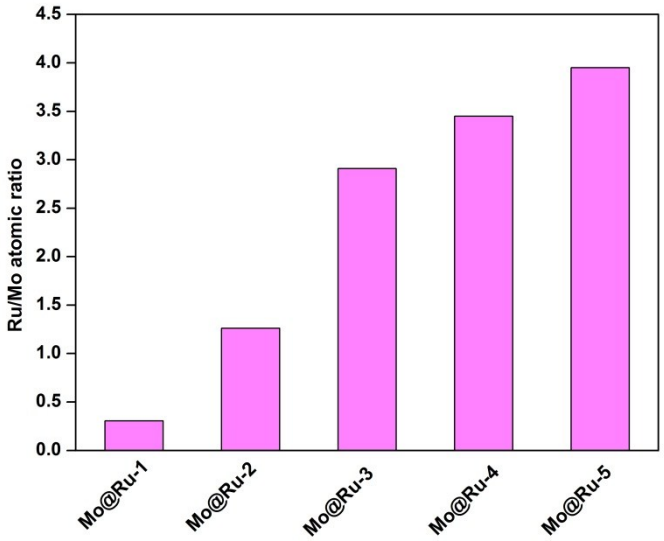

Figure S7. The Ru/Mo atomic ratio for Mo@Ru-x (x= 1 to 5) samples.

Table S2. Comparison of the overpotential at a current density of 10 mA cm^{-2} and Tafel slopes of Mo@Ru-3 in this work with other catalysts.

Catalyst	**Overpotential (mV)**	**Tafel slop (mV dec^{-1})**	**Reference**
Mo@Ru-3	30.5	36.4	This work
Ru nanosheets	20	46	[1]
Ru@C_2N	22	30	[2]
Ru/layered carbon	35	46	[3]
Ru/CCS	27.3	33	[4]
$Ni_{43}Ru_{57}$	41	31	[5]
NiRu@N–C	50	36	[6]
Ni@Ni_2P−Ru	51	35	[7]
Ru/grapphene	53	44	[8]
$WO_{0.29}$	70	50	[9]
Ni-Mo_2C@C	72	65.6	[10]
Ru/MeOH/THF	83	46	[11]
Fe_3C/Mo_2C@NPGC	98	45.2	[12]
WC nanoparticles	98	52	[13]
Mo_2C/graphene	130	57.3	[14]
Cu_7S_4@MoS_2	133	48	[15]
Co/CoP	146	51.3	[16]
1T-WS2	142	70	[17]
WC@CNTs	145	72	[18]
Co_2P	134	51.7	[19]
Co@Mo_2C	140	39	[20]
CoP	159	59	[21]
Co-NG	147	82	[22]
Mo_2C@PC	177	96	[23]

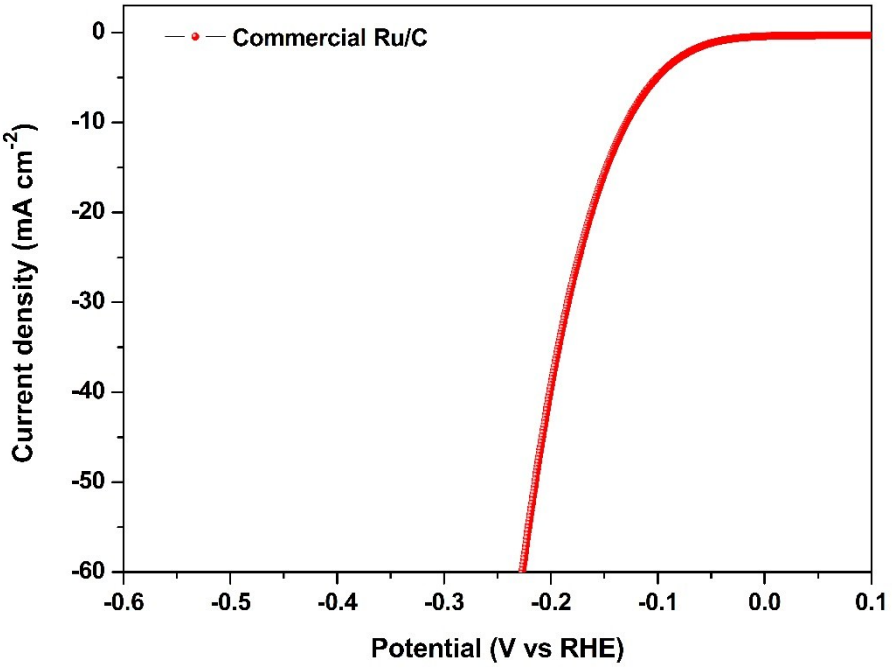

Figure S8. Polarization curve of commercial Ru/C (10 wt%) catalyst obtained in a three-electrode system. This catalyst requires 126.6 and 226.9 mV to drive the current densities of 10 and 60 mA cm^{-2}, respectively.

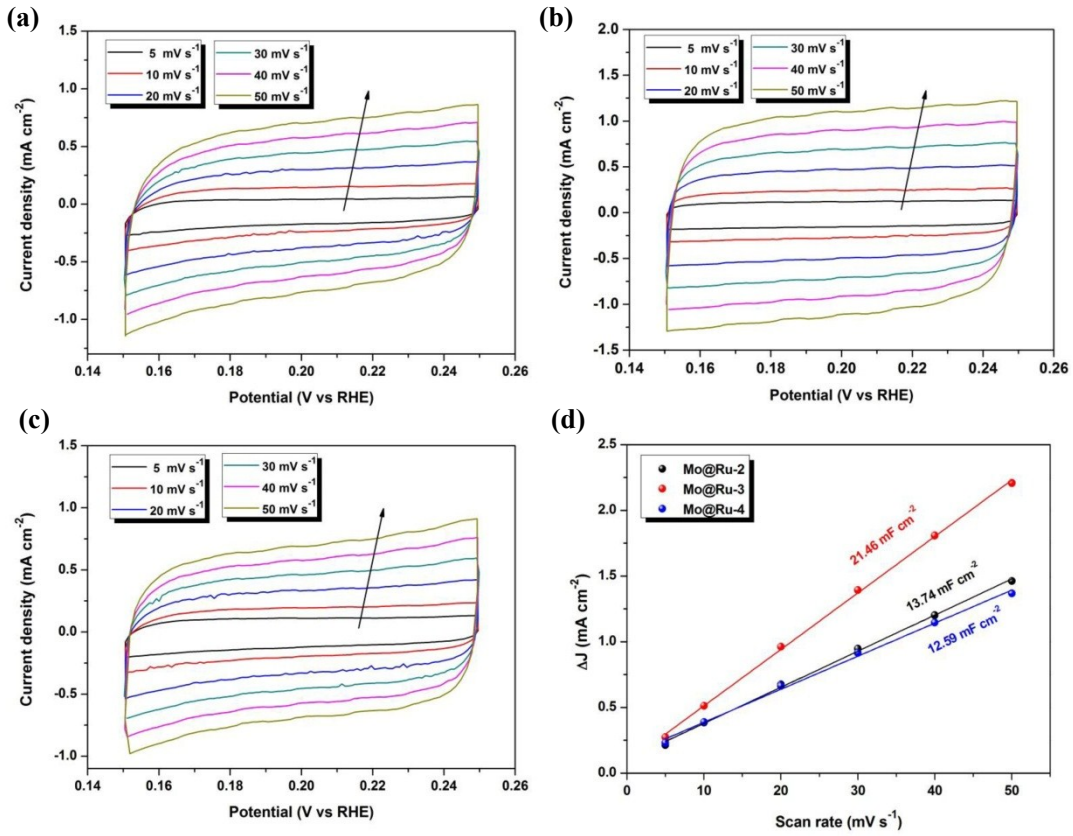

Figure S9. (a-c) Cyclic voltammetry curves of Mo@Ru-2, Mo@Ru-3 and Mo@Ru-4, respectively. The black arrow indicates the scan rate from 5 mV s^{-1} to 50 mV s^{-1}. (d) The current density variation (∆J =Ja-Jc) at an overpotential of 0.20 V plotted against scan rate fitted to a linear regression enables the estimation of C_{dl}, where the slope is twice C_{dl}.

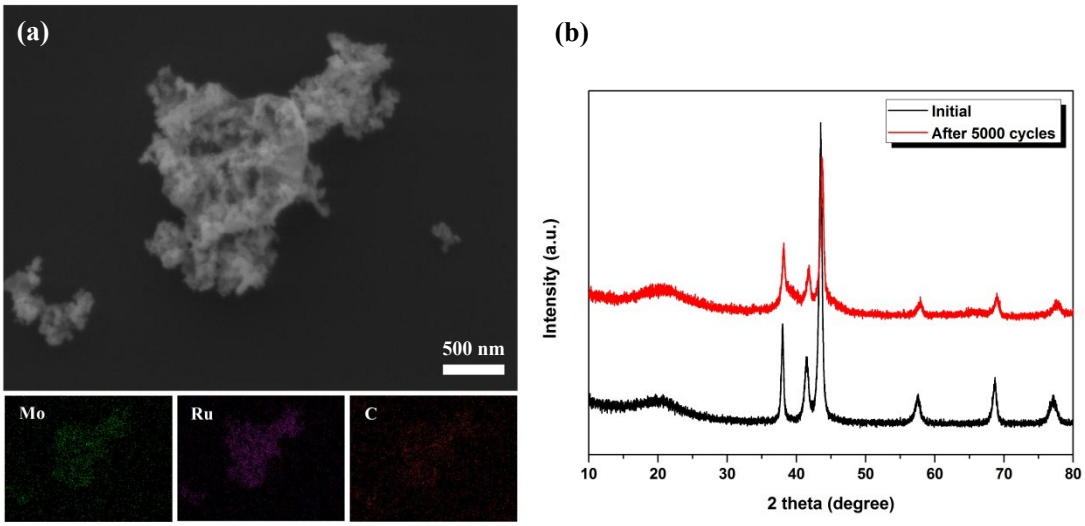

Figure S10. (a) SEM and EDS mapping, (b) XRD patterns for Mo@Ru-3 sample after 5000 CV cycles testing.

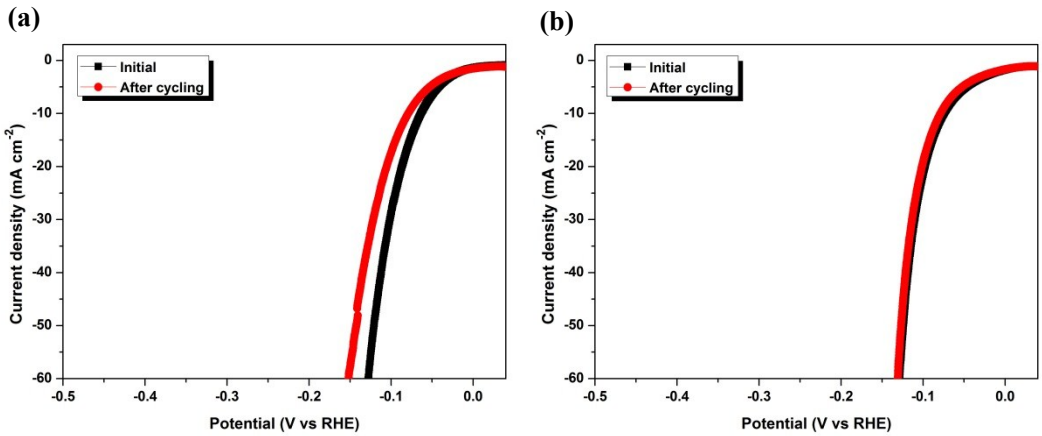

Figure S11. Polarization curves of (a) Mo@Ru-2 and Mo@Ru-4, respectively, recorded before and after 5000 potential sweeps.

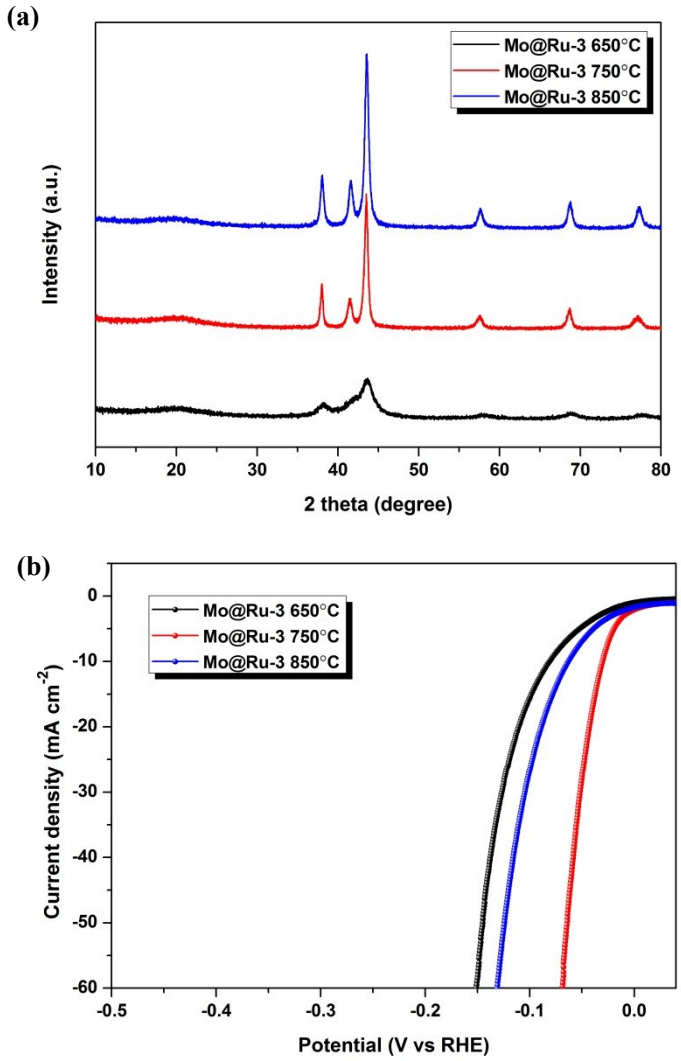

Figure S12. (a) XRD patterns and (b) HER polarization curves for Mo@Ru-3 samples annealed at 650°C, 750°C and 850°C, respectively.

Table S3. Current densities at various cell voltages and different temperatures for the as-prepared Mo@Ru-3 catalyst tested in a home-made PEM electrolyzer.

Current density (A cm^{-2})	1.6 V	1.7 V	1.8 V	1.9 V	2.0 V
25°C	0.026	0.103	0.213	0.354	0.502
40°C	0.041	0.145	0.288	0.461	0.645
60°C	0.070	0.216	0.403	0.627	0.865
80°C	0.120	0.319	0.564	0.852	1.156

Reference

1. X. Kong, K. Xu, C. Zhang, J. Dai, S. Norooz Oliaee, L. Li, X. Zeng, C. Wu and Z. Peng, *ACS Catal.*, 2016, **6**, 1487-1492.
2. J. Mahmood, F. Li, S. M. Jung, M. S. Okyay, I. Ahmad, S. J. Kim, N. Park, H. Y. Jeong and J. B. Baek, *Nat. Nanotechnol.*, 2017, **12**, 441-446.
3. Z. Chen, J. Lu, Y. Ai, Y. Ji, T. Adschiri and L. Wan, *ACS Appl. Mater. Interfaces*, 2016, **8**, 35132-35137.
4. D. Luo, B. Zhou, Z. Li, X. Qin, Y. Wen, D. Shi, Q. Lu, M. Yang, H. Zhou and Y. Liu, *Journal of Materials Chemistry A*, 2018, **6**, 2311-2317.
5. C. Zhang, Y. Liu, Y. Chang, Y. Lu, S. Zhao, D. Xu, Z. Dai, M. Han and J. Bao, *ACS Appl. Mater. Interfaces*, 2017, **9**, 17326-17336.
6. Y. Xu, S. Yin, C. Li, K. Deng, H. Xue, X. Li, H. Wang and L. Wang, *Journal of Materials Chemistry A*, 2018, **6**, 1376-1381.
7. Y. Liu, S. Liu, Y. Wang, Q. Zhang, L. Gu, S. Zhao, D. Xu, Y. Li, J. Bao and Z. Dai, *J. Am. Chem. Soc.*, 2018, **140**, 2731-2734.
8. R. Ye, Y. Liu, Z. Peng, T. Wang, A. S. Jalilov, B. I. Yakobson, S. H. Wei and J. M. Tour, *ACS Appl. Mater. Interfaces*, 2017, **9**, 3785-3791.
9. Y. H. Li, P. F. Liu, L. F. Pan, H. F. Wang, Z. Z. Yang, L. R. Zheng, P. Hu, H. J. Zhao, L. Gu and H. G. Yang, *Nat. Commun.*, 2015, **6**, 8064.
10. F. Yu, Y. Gao, Z. Lang, Y. Ma, L. Yin, J. Du, H. Tan, Y. Wang and Y. Li, *Nanoscale*, 2018, **10**, 6080-6087.
11. S. Drouet, J. Creus, V. Colliere, C. Amiens, J. Garcia-Anton, X. Sala and K. Philippot, *Chem Commun (Camb)*, 2017, **53**, 11713-11716.
12. J.-S. Li, Y.-J. Tang, C.-H. Liu, S.-L. Li, R.-H. Li, L.-Z. Dong, Z.-H. Dai, J.-C. Bao and Y.-Q. Lan, *Journal of Materials Chemistry A*, 2016, **4**, 1202-1207.
13. R. Ma, E. Song, Y. Zhou, Z. Zhou, G. Liu, Q. Liu, J. Liu, Y. Zhu and J. Wang, *Energy Storage Materials*, 2017, **6**, 104-111.
14. L. F. Pan, Y. H. Li, S. Yang, P. F. Liu, M. Q. Yu and H. G. Yang, *Chem Commun (Camb)*, 2014, **50**, 13135-13137.
15. J. Xu, J. Cui, C. Guo, Z. Zhao, R. Jiang, S. Xu, Z. Zhuang, Y. Huang, L. Wang and Y. Li, *Angew Chem Int Ed Engl*, 2016, **55**, 6502-6505.
16. Y. Li, H. Li, K. Cao, T. Jin, X. Wang, H. Sun, J. Ning, Y. Wang and L. Jiao, *Energy Storage Materials*, 2018, **12**, 44-53.
17. M. A. Lukowski, A. S. Daniel, C. R. English, F. Meng, A. Forticaux, R. J. Hamers and S. Jin, *Energy Environ. Sci.*, 2014, **7**, 2608-2613.
18. X. Fan, H. Zhou and X. Guo, *ACS Nano*, 2015, **9**, 5125-5134.
19. Z. Huang, Z. Chen, Z. Chen, C. Lv, M. G. Humphrey and C. Zhang, *Nano Energy*, 2014, **9**, 373-382.
20. H. Lin, N. Liu, Z. Shi, Y. Guo, Y. Tang and Q. Gao, *Adv. Funct. Mater.*, 2016, **26**, 5590-5598.
21. M. Liu and J. Li, *ACS Appl. Mater. Interfaces*, 2016, **8**, 2158-2165.
22. H. Fei, J. Dong, M. J. Arellano-Jimenez, G. Ye, N. Dong Kim, E. L. Samuel, Z. Peng, Z. Zhu, F. Qin, J. Bao, M. J. Yacaman, P. M. Ajayan, D. Chen and J. M. Tour, *Nat. Commun.*, 2015, **6**, 8668.

23. J. Yang, F. Zhang, X. Wang, D. He, G. Wu, Q. Yang, X. Hong, Y. Wu and Y. Li, *Angew Chem Int Ed Engl*, 2016, **55**, 12854-12858.